European Journal of Pharmacology 655 (2011) 31–37

Contents lists available at ScienceDirect

European Journal of Pharmacology

journal homepage: www.elsevier.com/locate/ejphar

Neuropharmacology and Analgesia

Allyl isothiocyanates and cinnamaldehyde potentiate miniature excitatory postsynaptic inputs in the supraoptic nucleus in rats

Toru Yokoyama [a,b], Toyoaki Ohbuchi [a], Takeshi Saito [a], Yuka Sudo [b,c], Hiroaki Fujihara [a], Kouichiro Minami [a,b], Toshihisa Nagatomo [a], Yasuhito Uezono [b], Yoichi Ueta [a,*]

[a] Department of Physiology, School of Medicine, University of Occupational and Environmental Health, Kitakyushu 807-8555, Japan
[b] Cancer Pathophysiology Division, National Cancer Center Reseach Institute, Tokyo 104-0045, Japan
[c] Department of Molecular and Cellular Biology, Nagasaki University School of Biomedical Science, Nagasaki 852-8523, Japan

ARTICLE INFO

Article history:
Received 2 July 2010
Received in revised form 11 January 2011
Accepted 12 January 2011
Available online 23 January 2011

Keywords:
TRPA1
EPSC
IPSC
Slice patch clamp
Supraoptic nucleus

ABSTRACT

Allyl isothiocyanates (AITC) and cinnamaldehyde are pungent compounds present in mustard oil and cinnamon oil, respectively. These compounds are well known as transient receptor potential ankyrin 1 (TRPA1) agonists. TRPA1 is activated by low temperature stimuli, mechanosensation and pungent irritants such as AITC and cinnamaldehyde. TRPA1 is often co-expressed in TRPV1. Recent study showed that hypertonic solution activated TRPA1 as well as TRPV1. TRPV1 is involved in excitatory synaptic inputs to the magnocellular neurosecretory cells (MNCs) that produce vasopressin in the supraoptic nucleus (SON). However, it remains unclear whether TRPA1 may be involved in this activation. In the present study, we examined the role of TRPA1 on the synaptic inputs to the MNCs in *in vitro* rat brain slice preparations, using whole-cell patch-clamp recordings. In the presence of tetrodotoxin, AITC (50 μM) and cinnamaldehyde (30 μM) increased the frequency of miniature excitatory postsynaptic currents without affecting the amplitude. This effect was significantly attenuated by previous exposure to ruthenium red (10 μM), non-specific TRP channels blocker, high concentration of menthol (300 μM) and HC-030031 (10 μM), which are known to antagonize the effects of TRPA1 agonists. These results suggest that TRPA1 may exist at presynaptic terminals to the MNCs and enhance glutamate release in the SON.

1. Introduction

Allyl isothiocyanates (AITC) and cinnamaldehyde are pungent compounds present in mustard oil and cinnamon oil, respectively (Jordt et al., 2004; Bandell et al., 2004). Transient receptor potential ankyrin 1 (TRPA1) (formerly ANKTM1) is the only mammalian member of the TRPA subfamily, and belongs to the TRP superfamily (Story et al., 2003). TRPA1 is a non-selective cation channel expressed widely, encompassing 20–35% of sensory neurones (Jordt et al., 2004; Nagata et al., 2005). TRPA1 is activated by a variety of noxious stimuli, including cold temperatures (below 17 °C), alkaline pH (Story et al., 2003; Fujita et al., 2008) and mechanosensation (Kwan et al., 2006, 2009). Surprisingly, a recent study demonstrated that hypertonic solution activates TRPA1 channels in human embryonic kidney 293 cells transiently expressing rat TRPA1 (Zhang et al., 2008).

TRPA1 is found in a subset of primary sensory neurons of dorsal root ganglia (DRG) that coexpressed with noxious heat-sensing TRPV1 (Story et al., 2003; Kobayashi et al., 2005). A recent finding has indicated that an N-terminal variant of the TRPV1 channel is required for osmosensory transduction in mouse supraoptic nucleus (SON) neurones (Sharif Naeini et al., 2006). The release of arginine vasopressin (AVP) from the magnocellular neurosecretory cells (MNCs) in the SON is crucial for body fluid homeostasis. The neuronal activity of the MNCs and AVP release is modulated by excitatory and inhibitory synaptic inputs and humoral factors such as osmotic change in plasma and many different endogenous factors (Mason, 1980; Leng et al., 1982; Bourque, 1989; Nagatomo et al., 1995). Excitatory synaptic inputs to the SON in rats are activated by hyperosmotic stimulation (Inenaga et al., 1997). To our knowledge, it is unknown whether TRPA1 is involved in modulating excitatory and inhibitory synaptic inputs to the SON or whether TPPA1 expresses in the SON. Therefore, we examined the effects of AITC and cinnamaldehyde on excitatory and inhibitory synaptic inputs in the SON in rats.

2. Materials and methods

2.1. Animals

Experiments were performed on male Wistar rats weighting 100–200 g. All procedures described in the present study were carried out

* Corresponding author at: Department of Physiology, School of Medicine, University of Occupational and Environmental Health, 1-1 Iseigaoka, Yahatanishi-ku, Kitakyushu, 807-8555, Japan. Tel.: +81 93 691 7420; fax: +81 93 692 1711.
E-mail address: yoichi@med.uoeh-u.ac.jp (Y. Ueta).

0014-2999/$ – see front matter © 2011 Elsevier B.V. All rights reserved.
doi:10.1016/j.ejphar.2011.01.011

in accordance with the guidelines on the use and care of laboratory animals as set out by the Physiological Society of Japan and under the control of the Ethics Committee of Animal Care and Experimentation, University of Occupational and Environmental Health, Japan.

2.2. Slice preparations

Rats were sacrificed by decapitation. We ensured the absence of gross contusion and hemorrhage after removal of each brain from the skull. The brains were rapidly removed and cooled in a perfusion medium at 4 °C for 1 min. A block containing the hypothalamus was cut and glued to the stage of a vibratome-type slicer (DSK Linearslicer™ PRO7; DSK, Kyoto, Japan). After careful removal of the meninges, coronal slices (150-μm thick) containing the SON were cut as described previously (Nagatomo et al., 1995). The slices were carefully trimmed with a circular punch (inner diameter 1.8 mm) and preincubated in the perfusion medium at room temperature for at least 1 h, after which they were transferred to the recording chamber.

2.3. Solutions and drugs

The perfusion medium contained (in mM): NaCl 124; KCl 5; KH_2PO_4 1.24; $CaCl_2$ 2; $NaHCO_3$ 25.9; and glucose 10. For Ca^{2+}-free solution, Ca^{2+} was replaced by Mg^{2+} and the osmolality was adjusted by lowering the Na^+ concentration. The pH was adjusted to 7.3, and the osmolality of all the solutions ranged between 298 and 303 mOsmol/kg. AITC was purchased from Wako (Osaka, Japan). Cinnamaldehyde, HC-030031 and ruthenium red were purchased from Sigma (St. Louis, MO, USA). Tetrodotoxin (TTX) was obtained from Sankyo Co. (Tokyo, Japan). Menthol was purchased from Nacalai (Kyoto, Japan). For stock solution, AITC, cinnamaldehyde and HC-030031 were dissolved in dimethyl sulfoxide (DMSO). Menthol was dissolved in ethanol. TTX and ruthenium red were dissolved in distilled water, and then all the drugs were dissolved into a working solution, with the final concentration of the solvents not being more than 0.1%. All the solutions used in this experiment were bubbled with a mixture of 95% O_2–5% CO_2. The pipette solution used in the recording electrodes contained (in mM): K-gluconate 140; $MgCl_2$ 1, $CaCl_2$ 1; EGTA 10; and Mg-ATP 2 (pH 7.3 with Tris base). TTX was present in all experiments except for Ca^{2+}-free solution.

2.4. Whole-cell recordings and data analyses

The slices were fixed in a recording chamber as described previously (Kabashima et al., 1997). Briefly, the slices were placed onto a glass-bottomed chamber and fixed with a grid of parallel nylon threads supported by a U-shaped stainless steel weight. The volume of the recording chamber was 1 ml, and the perfusion rate was 1.4 ml/min. The solution level was kept constant by a low-pressure aspiration system. To identify magnocellular neurones in the SON, we used an upright microscope (BX-50, Olympus, Japan) with Nomarski optics (×400). The drugs were applied to the slice preparation by switching the perfusion solution using a two-way valve (HV 4-4, Hamilton, Reno, NV, USA). The dead space washing time was excluded from the calculations.

The electrodes used in this study were triple-pulled with a puller (P-87, Sutter Instrument Co., Novoto, CA, USA) from a glass capillary, and had a final resistance of 5–9 MΩ when filled with the electrode solution. Electrophysiological recordings were carried out at 32–33 °C. Whole-cell recordings were made from microscopically identified SON neurones in the upper surface layers of the slices. Recordings of postsynaptic currents began 5 min after membrane rupture when the current reached a steady state. Currents and voltages were recorded with an EPC-10 amplifier (HEKA, Lambrecht, Germany). Signals were filtered at 3 kHz, digitised at 1 kHz with an analogue-to-digital converter (Mac lab/v. 3.5, Castle Hill, NSW, Australia), and stored on the hard disk of a personal computer. For quantitative analysis of the synaptic currents, only the AC components (using a 1-Hz high pass filter) were used for analysis with software (AxoGraph V.3.6.1, Axon Instruments, Foster Hill, CA, USA). Spontaneous events were automatically screened using an amplitude threshold of 15 pA and then were visually accepted or rejected based on the rise time and decay time. Recordings included for data analysis were collected during periods of stable series resistance (10–20 MΩ with no compensation).

2.5. Statistical analysis

Data are expressed as mean ± S.E.M. with n representing the number of neurones tested. Differences between two groups were examined for statistical significance using the paired t-test and between multiple groups by one-way ANOVA. A P value less than 0.05 denoted the presence of a statistically significant difference.

3. Results

Spontaneous synaptic currents were recorded from a total of 97 MNCs that were identified microscopically in thin punch-out SON slice preparations from 42 rats. As reported previously (Kabashima et al., 1997), excitatory postsynaptic currents (EPSCs) and inhibitory postsynaptic currents (IPSCs) were observed under basal conditions (without any stimulus). The EPSCs and IPSCs could be recorded selectively by setting the holding potential at −70 mV for the EPSCs and at −20 mV for the IPSCs. The EPSCs were abolished by the application of 6-cyano-7-nitroquin-oxaline-2,3-dione (CNQX; a blocker of non-NMDA receptors), and the IPSCs were abolished by the application of picrotoxin (a blocker of $GABA_A$ receptor-gated Cl^- channels), indicating that EPSCs and IPSCs reflect glutamate and GABA release, respectively. Spontaneous EPSCs and IPSCs (sEPSCs and sIPSCs) were insensitive to the Na^+ channel blocker TTX (1 μM), indicating that the sEPSCs and sIPSCs recorded from the thin punch-out slice preparations were miniature EPSCs and miniature IPSCs (mEPSCs and mIPSCs) that reflected the spontaneous quantal release of glutamate and GABA, respectively.

3.1. The effects of AITC and cinnamaldehyde on the mEPSCs

For this analysis, the mEPSCs recorded during 3-min periods under and after the application of AITC and cinnamaldehyde were compared with the mEPSCs recorded during 3-min periods before AITC and cinnamaldehyde application. AITC (50 μM) potentiated the mEPSCs frequency significantly (149 ± 4.6% of control, $P<0.01$, $n=9$). The effects of AITC were selective on the frequency of the mEPSCs, and the amplitude remained virtually unaffected (99.6 ± 1.4% of control, $P>0.05$, $n=9$) (Fig. 1). AITC significantly potentiated the frequency of the mEPSCs in a dose-dependent manner when tested at three concentrations (10, 30 and 50 μM) (Fig. 3A). AITC increased the mEPSC frequency to 106 ± 4.7%, 133 ± 7.8% and 149 ± 4.6% of the control values (n = 5–9). The increases of mEPSC were significant at 30 μM and 50 μM. The application of cinnamaldehyde (30 μM) significantly increased the frequency of the mEPSCs without affecting the amplitude, like AITC (frequency 143 ± 9.1% of control, $P<0.01$, $n=9$, amplitude 100 ± 1.5% of control, $P>0.05$, $n=9$) (Fig. 2). Like AITC, cinnamaldehyde also significantly potentiated the frequency of the mEPSCs in a dose-dependent manner when tested at three concentrations (10, 20 and 30 μM) (Fig. 2B). Cinnamaldehyde increased the mEPSC frequency to 102 ± 4.1%, 127 ± 8.2% and 143 ± 9.1% of the control values (n = 5–9). The increases of mEPSC were significant at 20 μM and 30 μM.

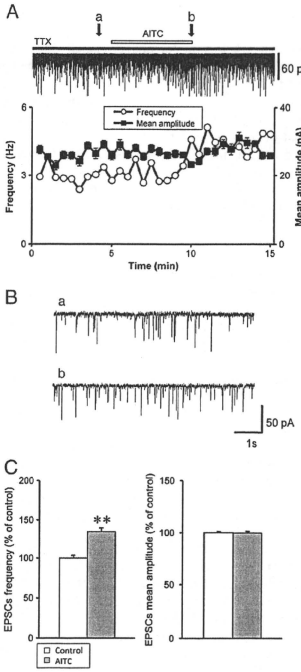

Fig. 1. Effect of AITC and related substances on miniature excitatory postsynaptic currents (mEPSCs) in the SON. (A) Representative example of AITC (50 μM) on mEPSCs. EPSCs were recorded in the presence of TTX (1 μM). The holding potential was −70 mV. Plots of frequency are single measurement, whereas plots of amplitude are mean ± S.E.M. over 30 s. (B) Consecutive trace of mEPSCs is shown in an expanded scale in time, (a) before and (b) during the action of AITC. (C) Summary of the effect of AITC on the frequency and amplitude of mEPSCs ($n=9$). The values are percentage changes (±S.E.M.) from control values obtained during a 3-min period at the beginning of the experiments (before adding AITC). **$P<0.01$ versus control.

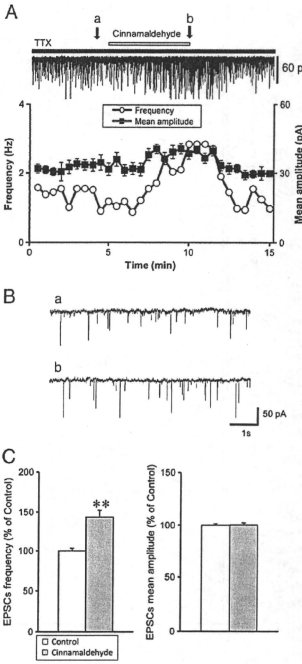

Fig. 2. Effect of cinnamaldehyde and related substances on miniature excitatory postsynaptic currents (mEPSCs) in the SON. (A) Representative example of cinnamaldehyde (30 μM) on mEPSCs. EPSCs were recorded in the presence of TTX (1 μM). The holding potential was −70 mV. Plots of frequency are single measurement, whereas plots of amplitude are mean ± S.E.M. over 30 s. (B) Consecutive trace of mEPSCs is shown in an expanded scale in time, (a) before and (b) during the action of cinnamaldehyde. (C) Summary of the effect of cinnamaldehyde on the frequency and amplitude of mEPSCs ($n=9$). The values are percentage changes (±S.E.M.) from control values obtained during a 3-min period at the beginning of the experiments (before adding cinnamaldehyde). **$P<0.01$ versus control.

3.2. The effects of AITC and cinnamaldehyde on the mIPSCs

In contrast to the effect on the mEPSCs, the application of AITC (50 μM) did not have significant effects (frequency 102 ± 3.6%, amplitude 106 ± 3.6% of control, $P>0.05$, $n=7$) on mIPSCs. In the same way as AITC, cinnamaldehyde (30 μM) did not have significant effects on the mIPSCs (frequency 100 ± 2.3%, amplitude 101 ± 1.3% of control, $P>0.05$, $n=6$).

3.3. Effects of TRP blocker on AITC- and cinnamaldehyde-induced potentiation of mEPSCs

To examine whether the effects of AITC and cinnamaldehyde are mediated by TRP channels, we used 10 μM ruthenium red, a non-specific TRP channel blocker. Figs. 4A and 5A show the representative examples of the effects of ruthenium red. Pre-exposure to ruthenium red attenuated the potentiation of mEPSCs by AITC (50 μM) and cinnamaldehyde (30 μM). Figs. 4B and 5B show the summary data for the effects of ruthenium red on the amplitude and frequency. Ruthenium red almost completely abolished the AITC- and cinnamaldehyde-induced increase in mEPSCs frequency, but had no effect on the amplitude of mEPSCs (AITC: frequency 102 ± 8.1%, amplitude 103 ± 1.8% of control, $n=6$; cinnamaldehyde: frequency 103 ± 6.3%, amplitude 104 ± 1.9% of control, $n=6$). These results suggest the possible involvement of TRP channels in both AITC- and cinnamaldehyde-induced potentiation of the mEPSCs.

3.4. Effects of TRPA1 antagonists on AITC- and cinnamaldehyde-induced potentiation of mEPSCs

To determine whether the effects of AITC and cinnamaldehyde on the mEPSCs are involved in TRPA1, we examined the pre-exposure high concentration of menthol and HC-030031 on AITC- and cinnamaldehyde-induced potentiation of mEPSCs. A previous study demonstrated that a low concentration of menthol activates TRPA1

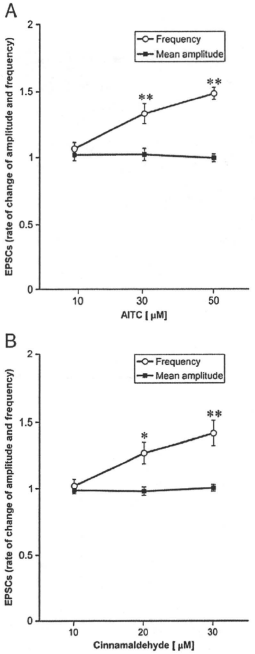

Fig. 3. Concentration–response relationship of AITC- and cinnamaldehyde-induced potentiation of miniature excitatory postsynaptic currents (mEPSCs). Supraoptic neurones were exposed to AITC at three different concentrations (10 μM, 30 μM and 50 μM; $n=5$–9) (A) or cinnamaldehyde at three different concentrations (10 μM, 20 μM and 30 μM; $n=5$–9), and the effects were expressed as rate of change (± S.E.M.) of frequency and amplitude of mEPSCs recorded for 3-min periods (after the start of AITC or cinnamaldehyde application) from value recorded in control periods before AITC application. Open circle, rate change of frequency; closed square, rate change of amplitude. *$P<0.05$ versus control and **$P<0.01$ versus control.

and a high concentration of menthol attenuates the effect of activation of TRPA1 (Karashima et al., 2007; Macpherson et al., 2006). Exposure to a high concentration of menthol (300 μM) did not affect the mEPSCs (frequency 99.0 ± 4.9%, amplitude 99.1 ± 1.9% of control. $n=6$). Pre-exposure to a high concentration of menthol attenuated the potentiation of mEPSCs by AITC (50 μM) and cinnamaldehyde (30 μM). High concentration of menthol almost abolished the AITC- and cinnamaldehyde-induced increase in the mEPSCs frequency, but had no effect on the amplitude of the mEPSCs (AITC: frequency 106 ± 8.6%, amplitude 103 ± 3.4% of control, $n=6$; cinnamaldehyde: frequency 103 ± 4.9%, amplitude 103 ± 1.6% of control, $n=3$) (Figs. 4C, D and 5C, D). HC-030031$_{(10\ \mu M)}$ also attenuated the AITC- and cinnamaldehyde-induced potentiation of mEPSCs (AITC: frequency 107 ± 4.1%, amplitude 102 ± 1.6% of control, $n=6$; cinnamaldehyde: frequency 107 ± 4.9%, amplitude 96.9 ± 1.6% of control, $n=6$) (Figs. 4E, F and 5E, F). These results suggest the possible involvement of TRPA1 channels in both AITC- and cinnamaldehyde-induced potentiation of the mEPSCs.

3.5. Effect of AITC on Ca^{2+}-free perfusion medium

To examine whether the potentiation of mEPSC by AITC is dependent on extracellular Ca^{2+}, we used Ca^{2+}-free solution. The frequency and amplitude of mEPSC in the Ca^{2+}-free solution were significantly smaller than that in normal perfusion solution (normal versus Ca^{2+}-free: frequency 1.67 ± 0.2 Hz versus 0.97 ± 0.1 Hz, $n=8$–9, $P<0.01$, amplitude 24.4 ± 0.4 pA versus 22.9 ± 0.3 pA, $n=8$–9, $P<0.05$). Under this condition, AITC did not increase the frequency and amplitude of mEPSC (frequency 105 ± 6.1% of control, amplitude 104 ± 1.8% of control, $n=8$) (Fig. 6). Thus, the AITC-induced potentiation of mEPSC was extracellular Ca^{2+}-dependent.

4. Discussion

In the present study, we provided the first evidence that AITC and cinnamaldehyde are well known as TRPA1 agonists potentiate excitatory synaptic inputs to the supraoptic MNCs in rats using a whole-cell patch-clamp technique. Because glutamate and GABA are two major synaptic inputs into the SON neurones (Meeker et al., 1993; Wuarin and Dudek, 1993), the potentiation of mEPSCs by TRPA1 agonists, AITC and cinnamaldehyde may, at least in part, account for the excitatory action on electrical activity. The mEPSCs recorded in the SON slice preparations that we employed in this study were virtually insensitive to TTX. This result suggests that TRPA1 modulates glutamate release from the presynaptic terminal, and that increases of EPSCs do not depend upon action potential. The neurones were recorded in thin SON slices containing only the SON and the perinuclear zone, and the mEPSCs and mIPSCs probably reflect spontaneous transmitter release from the terminals of the cut axons, disconnected from their cell origin.

TRPA1 is a non-selective cation channel and is activated by noxious cold, pungent natural compounds such as AITC and cinnamaldehyde, mechanosensation and alkaline pH (Story et al., 2003; Bandell et al., 2004; Fujita et al., 2008; Jordt et al., 2004; Kwan et al., 2006, 2009). Activation of the TRPA1 channel is reversibly blocked by a high concentration of menthol (Macpherson et al., 2006; Karashima et al., 2007; Xiao et al., 2008). Moreover, a recent study demonstrated that hypertonic solution activates TRPA1 channels in human embryonic kidney 293 cells transiently expressing rat TRPA1 (Zhang et al., 2008).

Plasma osmolality is well known to regulate the activity of MNCs (Mason, 1980; Leng et al., 1982; Bourque, 1989). The supraoptic MNCs receive synaptic inputs from the organum vasculosum lamina terminals, the median nucleus of the preoptic area and the subfronical organ (Chaudhry et al., 1989; Honda et al., 1990; Richard and Bourque, 1992; 1995). These areas are very sensitive to osmotic changes and regulate body fluid and drinking behaviour (Bourque et al., 1994). In addition to integrative information from the osmosensitive areas, the MNCs are themselves also osmosensitive (Mason, 1980; Oliet and Bourque, 1992, 1993). Hyperosmotic stimuli also directly modulate glutamatergic inputs to the supraoptic MNCs by acting on the presynaptic terminals (Inenaga et al., 1997). A recent finding has indicated that an N-terminal variant of TRPV1 channel is required for osmosensory transduction in mouse SON neurones (Sharif Naeini et al., 2006). TRPA1 is present in TRPV1-expressing sensory neurones (Story et al., 2003; Kobayashi et al., 2005). However, it is unknown whether TRPA1 expresses in the SON. Our present study demonstrated that TRPA1 agonists potentiate excitatory synaptic inputs and these effects were attenuated by a high concentration of menthol and HC-030031. The results of our studies did not contradict previous reports which provide the relationship with TRPA1 channel and menthol (Karashima et al., 2007; Macpherson et al., 2007a; Xiao et al., 2008). These results suggest that activation of the TRPA1 channel possibly potentiates the excitatory synaptic inputs to the supraoptic MNCs neurones. Formalin, known as TRPA1 agonist-induced nociceptive stimulation, causes a rapid elevation of AVP levels (Suzuki

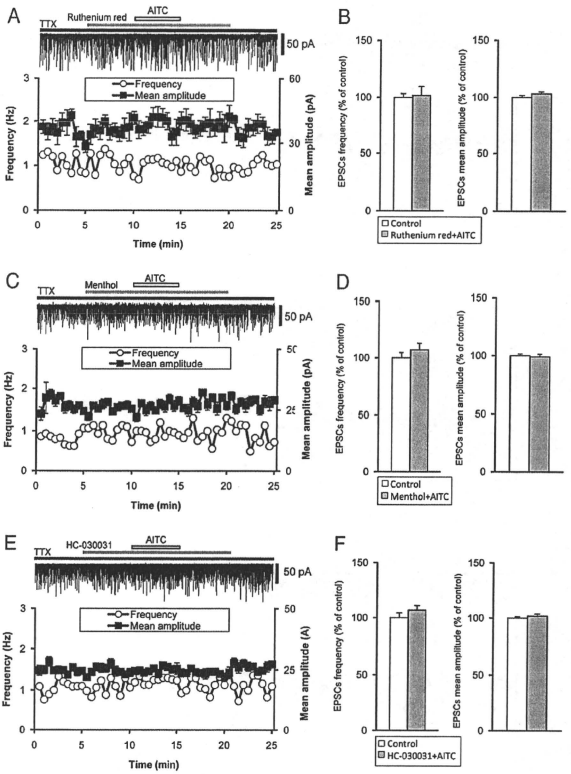

Fig. 4. Characterization of AITC-induced potentiation of mEPSCs. (A, C and E) Representative examples of the effects of ruthenium red (10 μM), non-specific TRP channels blocker (A), high concentration of menthol (300 μM) (C) and HC-030031 (10 μM) (E), TRPA1 selective channel blockers, on AITC-induced potentiation of mEPSCs. EPSCs were recorded in the presence of TTX (1 μM). The holding potential was −70 mV. Plots of frequency are single measurement, whereas plots of amplitude are mean ± S.E.M. over 30 s. (B, D and F) Summary data for characterization of mEPSCs under AITC (50 μM) application. Frequency (left) and amplitude (right) of mEPSCs. Ruthenium red plus AITC ($n=6$) (B), high concentration of menthol plus AITC ($n=6$) (D) and HC-030031 plus AITC ($n=6$) (F), respectively. Data are mean ± S.E.M.

et al., 2009). TRPA1 recognizes temperature and a chemical sense in the brain of the snake (Gracheva et al., 2010). The potentiation of excitatory synaptic transmission by the activation of presynaptic terminals TRPA1 may have an important role in neuronal activity and the secretion of neurohypophysial hormones (AVP and oxytocin (OXT)). It cannot be denied that extracellular matrixes around the MNCs, such as protein, glial cell and other mechano-channels, may participate in the regulation of glutamatergic release by TRPA1 agonists.

Previous studies have reported that noxious compounds such as AITC are activated through covalent modification of cysteine residues in the intercellular N-terminal domain (Hinman et al., 2006; Macpherson et al., 2007b), whereas activation by intercellular calcium appears to be dependent on the N-terminal EF-hand calcium-binding domain (Doerner et al., 2007; Zurborg et al., 2007). In the present study, AITC-induced potentiation of mEPSCs was attenuated under extracellular Ca^{2+} free solution. A recent study demonstrated that transmembrane domain 5 is a critical molecular determinant of menthol sensitivity in mammalian TRPA1 channels (Xiao et al., 2008). These results indicate that TRPA1 in the SON may be activated through covalent modification of cysteine residues in the N-terminal domain and by extracellular Ca^{2+}-dependent. However, it remains obscure what kind of physiological role TRPA1 mediates.

The MNCs (AVP- or OXT-producing neurones) in the SON can be divided into two groups based on their firing pattern. By combining immunohistochemical and electrophysiological techniques, most of the phasically firing neurones contain AVP (phasic neurones), whereas the other neurones that do not fire phasically (nonphasic neurones) contain OXT (Yamashita et al., 1983; Cobbett et al., 1986; Armstrong et al., 1994). A previous immunohistochemical study

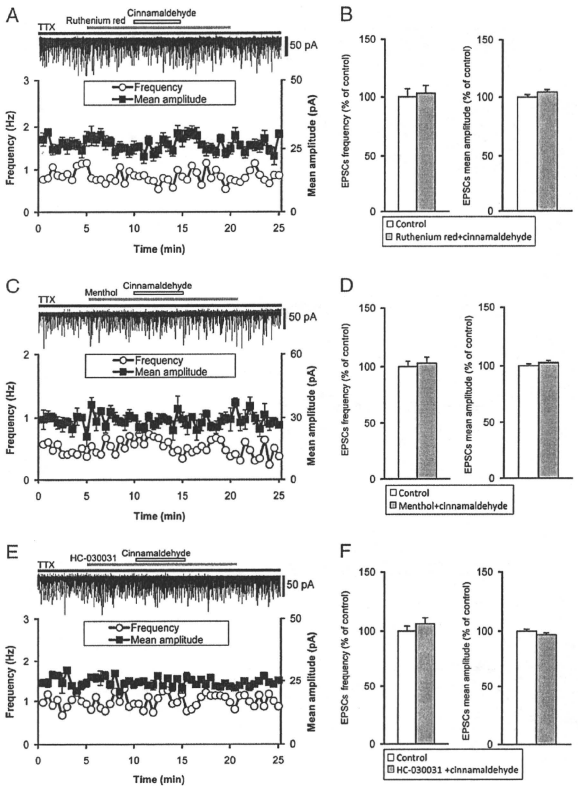

Fig. 5. Characterization of cinnamaldehyde-induced potentiation of mEPSCs. (A, C and E) Representative examples of the effects of ruthenium red (10 μM), non-specific TRP channels blocker (A), high concentration of menthol (300 μM) (C) and HC-030031 (10 μM) (E), TRPA1 selective channel blockers, on cinnamaldehyde-induced potentiation of mEPSCs. EPSCs were recorded in the presence of TTX (1 μM). The holding potential was −70 mV. Plots of frequency are single measurement, whereas plots of amplitude are mean ± S.E.M. over 30 s. (B, D and F) Summary data for characterization of mEPSCs under cinnamaldehyde (30 μM) application. Frequency (left) and amplitude (right) of mEPSCs. Ruthenium red plus cinnamaldehyde ($n=6$) (B), high concentration of menthol plus cinnamaldehyde ($n=3$) (D) and HC-030031 plus cinnamaldehyde ($n=6$) (F), respectively. Data are mean ± S.E.M.

demonstrated that AVP neurones are more common in the caudal and ventral parts of the SON, while OXT neurones tend to be found rostrally and dorsally (Rhodes et al., 1981). Subsequent topographic analysis revealed the majority of Fos-expressing AVP neurones occupy the ventral part of the SON, while Fos-OXT neurons are mainly in the dorsal part on hyperosmotic stimulation (Pirnik et al., 2004). We recorded mEPSCs in the ventral part of the SON. In the present study, approximately 75% of the tested supraoptic MNCs were sensitive to AITC and cinnamaldehyde. Taken together, and although we identified the cell types electrophysiologically, the possibility that the action of AITC and cinnamaldehyde is restricted to a single cell type (AVP- or OXT-producing neurones) is unlikely.

In conclusion, AITC and cinnamaldehyde potentiate excitatory synaptic inputs to the MNCs in the SON on electrophysiolgy. Additional investigations will be required to clarify the physiological role of TRPA1 in glutamatergic excitatory synaptic transmission in supraoptic MNCs.

Acknowledgements

This study was supported by Grant-in-Aids for Scientific Research on Priority Area No. 18077006 (Y. Ueta), Scientific Research (B) 22390044 (Y. Ueta) and Scientific Research (C) No. 20602019 (T. Yokoyama) from the Ministry of Education, Culture, Sports, Science and Technology, Japan, and this study was also supported by a Grant in-Aid for the Third Term Comprehensive 10-Year Strategy for Cancer Control and Cancer Research No. 21150801 (Y. Uezono), a Grant-in-Aid for Cancer Research (21-9-1) from the Japanese Ministry of Health, Labor and Welfare,

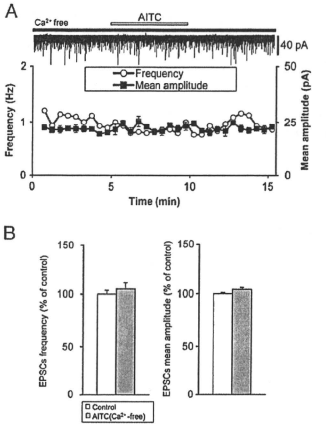

Fig. 6. AITC-induced potentiation of mEPSCs is extracellular Ca^{2+} dependent. (A) A representative example of the effect of AITC (50 μM) on AITC-induced potentiation of mEPSCs in the Ca^{2+}-free perfusion medium. (B) Summary data for the effects of AITC on frequency and amplitude of mEPSCs in Ca^{2+}-free solution ($n = 8$). Data are mean ± S.E.M.

Tokyo, Japan (Y. Uezono) and UOEH Grant for Advanced Research (Y. Ueta).

References

Armstrong, W.E., Smith, B.N., Tian, M., 1994. Electrophysiological characteristics of immunochemically identified rat oxytocin and vasopressin neurones in vitro. J. Physiol. 475, 115–128.

Bandell, M., Story, G.M., Hwang, S.W., Viswanath, V., Eid, S.R., Petrus, M.J., Earley, T.J., Patapoutian, A., 2004. Noxious cold ion channel TRPA1 is activated by pungent compounds and bradykinin. Neuron 41, 849–857.

Bourque, C.W., 1989. Ionic basis for the intrinsic activation of rat supraoptic neurones by hyperosmotic stimuli. J. Physiol. 417, 263–277.

Bourque, C.W., Oliet, S.H., Richard, D., 1994. Osmoreceptors, osmoreception, and osmoregulation. Front. Neuroendocrinol. 15, 231–274.

Chaudhry, M.A., Dyball, R.E., Honda, K., Wright, N.C., 1989. The role of interconnection between supraoptic nucleus and anterior third ventricular region in osmoregulation in the rat. J. Physiol. 410, 123–135.

Cobbett, P., Smithson, K.G., Hatton, G.I., 1986. Immunoreactivity to vasopressin- but not oxytocin-associated neurophysin antiserum in phasic neurons of rat hypothalamic paraventricular nucleus. Brain Res. 362, 7–16.

Doerner, J.F., Gisselmann, G., Hatt, H., Wetzel, C.H., 2007. Transient receptor potential channel A1 is directly gated by calcium ions. J. Biol. Chem. 282, 13180–13189.

Fujita, F., Uchida, K., Moriyama, T., Shima, A., Shibasaki, K., Inada, H., Sokabe, T., Tominaga, M., 2008. Intracellular alkalization causes pain sensation through activation of TRPA1 in mice. J. Clin. Invest. 118, 4049–4057.

Gracheva, E.O., Ingolia, N.T., Kelly, Y.M., Cordero-Morales, J.F., Hollopeter, G., Chesler, A.T., Sanchez, E.E., Perez, J.C., Weissman, J.S., Julius, D., 2010. Molecular basis of infrared detection by snakes. Nature 464, 1006–1011.

Hinman, A., Chuang, H.H., Bautista, D.M., Julius, D., 2006. TRP channel activation by reversible covalent modification. Proc. Natl. Acad. Sci. USA 103, 19564–19568.

Honda, K., Negoro, H., Higuchi, T., Takano, S., 1990. Activation of supraoptic neurosecretory cells by osmotic stimulation of the median preoptic nucleus. Neurosci. Lett. 119, 167–170.

Inenaga, K., Cui, L.N., Nagatomo, T., Honda, E., Ueta, Y., Yamashita, H., 1997. Osmotic modulation in glutamatergic excitatory synaptic inputs to neurons in the supraoptic nucleus of rat hypothalamus in vitro. J. Neuroendocrinol. 9, 63–68.

Jordt, S.E., Bautista, D.M., Chuang, H.H., McKemy, D.D., Zygmunt, P.M., Hogestatt, E.D., Meng, I.D., Julius, D., 2004. Mustard oils and cannabinoids excite sensory nerve fibres through the TRP channel ANKTM1. Nature 427, 260–265.

Kabashima, N., Shibuya, I., Ibrahim, N., Ueta, Y., Yamashita, H., 1997. Inhibition of spontaneous EPSCs and IPSCs by presynaptic GABAB receptors on rat supraoptic magnocellular neurons. J. Physiol. 504 (Pt 1), 113–126.

Karashima, Y., Damann, N., Prenen, J., Talavera, K., Segal, A., Voets, T., Nilius, B., 2007. Bimodal action of menthol on the transient receptor potential channel TRPA1. J. Neurosci. 27, 9874–9884.

Kobayashi, K., Fukuoka, T., Obata, K., Yamanaka, H., Dai, Y., Tokunaga, A., Noguchi, K., 2005. Distinct expression of TRPM8, TRPA1, and TRPV1 mRNAs in rat primary afferent neurons with adelta/c-fibers and colocalization with trk receptors. J. Comp. Neurol. 493, 596–606.

Kwan, K.Y., Allchorne, A.J., Vollrath, M.A., Christensen, A.P., Zhang, D.S., Woolf, C.J., Corey, D.P., 2006. TRPA1 contributes to cold, mechanical, and chemical nociception but is not essential for hair-cell transduction. Neuron 50, 277–289.

Kwan, K.Y., Lazer, J.M., Corey, D.P., Rice, D.P., Stucky, C.L., 2009. TRPA1 modulates mechanotransduction in cutaneous sensory neurons. J. Neurosci. 29, 4808–4819.

Leng, G., Mason, W.T., Dyer, R.G., 1982. The supraoptic nucleus as an osmoreceptor. Neuroendocrinology 34, 75–82.

Macpherson, L.J., Hwang, S.W., Miyamoto, T., Dubin, A.E., Patapoutian, A., Story, G.M., 2006. More than cool: promiscuous relationships of menthol and other sensory compounds. Mol. Cell. Neurosci. 32, 335–343.

Macpherson, L.J., Dubin, A.E., Evans, M.J., Marr, F., Schultz, P.G., Cravatt, B.F., Patapoutian, A., 2007a. Noxious compounds activate TRPA1 ion channels through covalent modification of cysteines. Nature 445, 541–545.

Macpherson, L.J., Xiao, B., Kwan, K.Y., Petrus, M.J., Dubin, A.E., Hwang, S., Cravatt, B., Corey, D.P., Patapoutian, A., 2007b. An ion channel essential for sensing chemical damage. J. Neurosci. 27, 11412–11415.

Mason, W.T., 1980. Supraoptic neurones of rat hypothalamus are osmosensitive. Nature 287, 154–157.

Meeker, R.B., Swanson, D.J., Greenwood, R.S., Hayward, J.N., 1993. Quantitative mapping of glutamate presynaptic terminals in the supraoptic nucleus and surrounding hypothalamus. Brain Res. 600, 112–122.

Nagata, K., Duggan, A., Kumar, G., Garcia-Anoveros, J., 2005. Nociceptor and hair cell transducer properties of TRPA1, a channel for pain and hearing. J. Neurosci. 25, 4052–4061.

Nagatomo, T., Inenaga, K., Yamashita, H., 1995. Transient outward current in adult rat supraoptic neurones with slice patch-clamp technique: inhibition by angiotensin II. J. Physiol. 485 (Pt 1), 87–96.

Oliet, S.H., Bourque, C.W., 1992. Properties of supraoptic magnocellular neurones isolated from the adult rat. J. Physiol. 455, 291–306.

Oliet, S.H., Bourque, C.W., 1993. Mechanosensitive channels transduce osmosensitivity in supraoptic neurons. Nature 364, 341–343.

Pirnik, Z., Miravec, B., Kiss, A., 2004. Fos protein expression in mouse hypothalamic paraventricular (PVN) and supraoptic (SON) nuclei upon osmotic stimulus: colocalization with vasopressin, oxytocin, and tyrosine hydroxylase. Neurochem. Int. 45, 597–607.

Rhodes, C.H., Morrel, J.I., Pfaff, D.M., 1981. Immunohistochemical analysis of magnocellular elements in rat hypothalamus: distribution and numbers of cells containing neurophysin, oxytocin, and vasopressin. J. Comp. Neurol. 198, 45–64.

Richard, D., Bourque, C.W., 1992. Synaptic activation of rat supraoptic neurons by osmotic stimulation of the organum vasculosum lamina terminalis. Neuroendocrinology 55, 609–611.

Richard, D., Bourque, C.W., 1995. Synaptic control of rat supraoptic neurones during osmotic stimulation of the organum vasculosum lamina terminalis in vitro. J. Physiol. 489 (Pt 2), 567–577.

Sharif Naeini, R., Witty, M.F., Seguela, P., Bourque, C.W., 2006. An N-terminal variant of Trpv1 channel is required for osmosensory transduction. Nat. Neurosci. 9, 93–98.

Story, G.M., Peier, A.M., Reeve, A.J., Eid, S.R., Mosbacher, J., Hricik, T.R., Earley, T.J., Hergarden, A.C., Andersson, D.A., Hwang, S.W., McIntyre, P., Jegla, T., Bevan, S., Patapoutian, A., 2003. ANKTM1, a TRP-like channel expressed in nociceptive neurons, is activated by cold temperatures. Cell 112, 819–829.

Suzuki, H., Kawasaki, M., Ohnishi, H., Otsubo, H., Ohbuchi, T., Katoh, A., Hashimoto, H., Yokoyama, T., Fujihara, H., Dayanithi, G., Murphy, D., Nakamura, T., Ueta, Y., 2009. Exaggerated response of a vasopressin-enhanced green fluorescent protein transgene to nociceptive stimulation in the rat. J. Neurosci. 29, 13182–13189.

Wuarin, J.P., Dudek, F.E., 1993. Patch-clamp analysis of spontaneous synaptic currents in supraoptic neuroendocrine cells of the rat hypothalamus. J. Neurosci. 13, 2323–2331.

Xiao, B., Dubin, A.E., Bursulaya, B., Viswanath, V., Jegla, T.J., Patapoutian, A., 2008. Identification of transmembrane domain 5 as a critical molecular determinant of menthol sensitivity in mammalian TRPA1 channels. J. Neurosci. 28, 9640–9651.

Yamashita, H., Inenaga, K., Kawata, M., Sano, Y., 1983. Phasically firing neurons in the supraoptic nucleus of the rat hypothalamus: immunocytochemical and electrophysiological studies. Neurosci. Lett. 37, 87–92.

Zhang, X.F., Chen, J., Faltynek, C.R., Moreland, R.B., Neelands, T.R., 2008. Transient receptor potential A1 mediates an osmotically activated ion channel. Eur. J. Neurosci. 27, 605–611.

Zurborg, S., Yurgionas, B., Jira, J.A., Caspani, O., Heppenstall, P.A., 2007. Direct activation of the ion channel TRPA1 by Ca2+. Nat. Neurosci. 10, 277–279.

Endocrine Journal 2010, **57** (9), 825-832

NOTE

Caspase 8 and menin expressions are not correlated in human parathyroid tumors

Dong Yu[1], Yuko Nagamura[1], Satoko Shimazu[1], Junko Naito[2], Hiroshi Kaji[2], Seiki Wada[3], Munehiro Honda[4], Lian Xue[5] and Toshihiko Tsukada[1]

[1]*Tumor Endocrinology Project, National Cancer Center Research Institute, Tokyo 104-0045, Japan*
[2]*Division of Diabetes and Endocrinology, Department of Internal Medicine, Kobe University Graduate School of Medicine, Kobe 650-0017, Japan*
[3]*Institute of Endocrine and Metabolic Disorders, Saitama 358-0011, Japan*
[4]*Department of Endocrinology and Metabolism, Mishuku Hospital, Tokyo 153-0051, Japan*
[5]*School of Radiation Medicine and Public Health, Medical College of Soochow University, Suzhou 215123, China*

Abstract. Menin is lost by the sequential inactivation of both *MEN1* alleles in subsets of non-hereditary endocrine tumors as well as those associated with multiple endocrine neoplasia type 1 (MEN1), an autosomal dominant hereditary cancer syndrome characterized by multiple tumors including parathyroid, pituitary and enteropancreatic endocrine tumors. Loss of menin has been reported to be associated with lowered caspase 8 expression and resistance to apoptosis in murine fibroblasts and in pancreatic islet tumors arising in heterozygous *MEN1* gene knockout mice, the animal model of the human MEN1 syndrome. We confirmed by menin-knockdown experiments with specific siRNA that menin is crucial for caspase 8 expression in human culture cells while overexpression of menin did not increase caspase 8 protein over basal levels. We then examined expression of menin, caspase 8 and cyclin-dependent kinase inhibitors $p27^{Kip1}$ and $p15^{Ink4b}$ by Western blotting in human parathyroid tumors surgically resected from patients with MEN1 and those with non-hereditary primary hyperparathyroidism. The menin and $p27^{Kip1}$ expression levels were correlated with *MEN1* mutation status that was confirmed by DNA analysis. The caspase 8 and $p15^{Ink4b}$ protein levels were variable among tumors, and were not correlated with menin protein levels. These findings suggest that human endocrine tumors lacking menin may not always exhibit lowered caspase 8 expression and hence may not be resistant to apoptosis-inducing therapy.

Key words: MEN1, Menin, Caspase 8, siRNA

MENIN is the protein product of the tumor suppressor gene *MEN1*, the causative gene of multiple endocrine neoplasia type 1 (MEN1), an autosomal dominant familial cancer syndrome characterized by the multiple occurrence of endocrine tumors, such as pituitary, parathyroid and pancreatic islet tumors [1, 2]. Following the inactivation of the both *MEN1* alleles, the wild-type menin is lost in the tumors associated with MEN1. Menin is also frequently lost in some non-hereditary, sporadic endocrine tumors by somatic mutations of the both *MEN1* alleles. For example, 21 % and 39 % of sporadic parathyroid tumors have been reported to exhibit somatic *MEN1* gene mutation and loss of heterozygosity (LOH) of the *MEN1* locus, respectively [3]. These findings suggest that the complete loss of menin is an important step in the development of not only hereditary but also subsets of sporadic endocrine tumors.

Menin is ubiquitously expressed and mainly targeted to the nucleus [4, 5]. Although its molecular function is not fully understood, menin has been shown to modify chromatin structure and thereby regulate the transcription of many target genes including cyclin-dependent kinase inhibitor (CDKI) genes $p18^{Ink4c}$ and $p27^{Kip1}$ [2, 6]. Menin-induced expression of these CDKI genes seems to be relevant to tumor suppressor function of menin because inactivating germline mutations of the CDKI genes $p15^{Ink4b}$, $p18^{Ink4c}$, $p21^{Cip1}$ and $p27^{Kip1}$ are known to cause MEN1-like syndromes [7, 8].

Received Mar. 19, 2010; Accepted Jun. 1, 2010 as K10E-085
Released online in J-STAGE as advance publication Jul. 3, 2010
Correspondence to: Toshihiko Tsukada, Tumor Endocrinology Project, National Cancer Center Research Institute, 5-1-1 Tsukiji, Chuo-ku, Tokyo 104-0045, Japan. E-mail: ttsukada@ncc.go.jp

On the other hand, previous studies have shown that menin plays a crucial role in promoting apoptosis, which depends on proapoptotic proteins of Bax and Bak [9]. Menin has also been demonstrated to induce the expression of caspase 8 mRNA and protein by enhancing histone acetylation at the 5'-untranslated region of the caspase 8 gene in murine embryonic fibroblasts [10]. Moreover, caspase 8 expression has been shown to decline in pancreatic islets and insulinomas in heterozygous *MEN1* gene knockout mice, the murine model of the human MEN1 syndrome [10]. These findings suggest that menin-dependent caspase 8 expression plays a role in tumor suppression. Because caspase 8 is a key protein in the death-receptor pathways, tumors lacking caspase 8 may be resistant to apoptosis-inducing therapy [11].

Although the endocrine tumors in the murine MEN1 model showed decreased caspase 8 expression, it remains uncertain whether the human endocrine tumors lacking menin exhibit similarly lowered caspase 8 levels. To clarify the relationships between caspase 8 and menin expression levels in human tumors, we have studied caspase 8 proteins in human culture cells and in parathyroid tumors associated with MEN1 and non-hereditary parathyroid tumors. We report here that caspase 8 expression was down-regulated by menin knockdown in human culture cells, but human parathyroid tumors had variable amounts of caspase 8 proteins irrespective of menin expression levels.

Materials and Methods

Cell culture and transfection of expression plasmid and siRNA

WI38-VA13 and GM0639 cells, the human fibroblasts derived from normal persons and immortalized with SV40, and HEK293T cells, the transformed human embryonic kidney cells, were maintained in DMEM supplemented with 10 % fetal bovine serum and antibiotics as described previously [12]. GM0639 cells were treated with 50 μM etoposide for 48 h to be served as a control for procaspase and cleaved caspase proteins in Western blotting.

The menin-expressing plasmid was constructed by inserting the protein-coding region of the menin cDNA plasmid (p1533, kindly donated by Dr. M. Ohki and Dr. F. Hosoda, National Cancer Center Research Institute, Japan) into the unique *Hind*III site of the pRc/CMV expression vector (Invitrogen, USA) after blunting each end as described previously [5] . The plasmid was transfected with FuGENE6 transfection reagent (Roche, USA) and were harvested 48 h after transfection.

Menin siRNA or scrambled negative control siRNA (menin siRNA (h), sc-35922 and control siRNA-A, sc-37007, Santa Cruz Biotechnology, USA) were transfected by the procedures recommended by the supplier into culture cells that were seeded at 5×10^5 cells per 35 mm plate the day before transfection. After transfection, cells were cultured in normal growth media for 48 h before collection.

Real-time RT-PCR

Total RNA was extracted from cells with the RNeasy Mini Kit (Qiagen, USA). Specific mRNA was quantified by real-time PCR using a Fluorescent Quantitative Detection system (BioFlux, USA) with QuantiTect SYBR Green RT-PCR assay kits (Qiagen). The mRNA value for each gene was normalized relative to the human glyceraldehyde-3-phosphate dehydrogenase (GAPDH) mRNA levels in RNA samples. The following PCR primers were used for each mRNA. Menin: sense, TTAGGGAACCTGGCAGATCTAGAG; antisense, GTAGCCAGCCAGGTACATGTAGG; GAPDH: sense, TGCACCACCAACTGCTTAGC; antisense, AGTGATGGCATGGACTGTGG. Statistical comparison of mean values was performed by the Student's *t*-test. Differences with a p value of less than 0.05 were considered statistically significant.

Western blotting

Whole cell lysates were prepared as described previously [12]. Protein samples separated by electrophoresis and blotted onto nitrocellulose membrane (Invitrogen) were subjected to antibody binding as described previously [13]. The following antibodies were used: goat polyclonal anti-menin (C-19, sc-8200), rabbit polyclonal anti-$p27^{Kip1}$ (C-19, sc-528), rabbit polyclonal ant-$p15^{Ink4b}$ (K-18, sc-613), anti-mouse IgG-HRP and anti-goat IgG-HRP antibodies were purchased from Santa Cruz Biotechnology. Mouse monoclonal anti-actin antibody (clone C4, #MAB1501) was obtained from Millipore (USA). Mouse monoclonal anti-caspase 8 antibody (12F5, ALX-804-242) was provided by ENZO Life Sciences (USA). The blots were visualized by

Table 1 Parathyroid tumors examined.

Parathyroid Tumor	Germline *MEN1* mutation#	Predicted effect of germline mutation	LOH	Clinical features
1	c.1628C>G	S543X (termination at codon 543)	+	Recurrent parathyroid tumors
2*	c.893delC	frame shift at codon 298	+	Multiple parathyroid tumors, Gastrinoma; Familial
3	c.1072G>T	E358X (termination at codon 358)	ND	Multiple parathyroid tumors, Glucagonoma, Prolactinoma; Familial
4a, 4b	c.492delC	frame shift at codon 164	+	Recurrent parathyroid tumors, Acromegaly
5	c.1350+1_1350+14 del14insCT	abnormal splicing at the 3' end of exon 9	+	Familial hyperparathyroidism
6*	large deletion	gene deletion	+	Multiple parathyroid tumors, Gastrinoma, Adrenocortical tumor; Familial
7-12	none	-	ND	Sporadic parathyroid tumor

Tumors 4a and 4b are from different parathyroid glands of a single patient.
#, Mutations are designated by the standard nomenclature [19]. *, reported previously [20, 21]. ND, not determined.

enhanced chemiluminescence method (RPN2135, GE Healthcare, UK) and imaging system LAS3000 (Fujifilm, Japan). Images were analyzed with the ImageJ software.

Blood and tumor specimens

Patients with primary hyperparathyroidism were diagnosed as having non-hereditary, sporadic parathyroid tumor or hereditary tumors in the local hospitals (Table 1). The diagnosis of MEN1 was confirmed by DNA analysis for heterozygous germline *MEN1* gene mutation. Seven parathyroid tumors surgically removed from 6 patients affected with MEN1, including 2 tumors arising from different parathyroid glands of a patient (case 4), and 6 parathyroid tumors from 6 patients with non-hereditary, sporadic parathyroid tumor were examined. The tumors were pathologically diagnosed as benign multiple adenomas or hyperplasia in the MEN1 cases and as benign adenoma in sporadic cases.

Peripheral blood was collected from all MEN1 patients except for one patient (case 3) and used for the confirmation of germline mutation and LOH analysis. Prior informed consent was obtained for germline mutation analysis of blood DNA. Some tumors were analyzed after unlinkable anonymization without informed consent for gene analysis. This study was approved by the ethics committee for gene analysis research of the National Cancer Center and Kobe University Graduate School of Medicine.

Analysis of MEN1 gene mutation and loss of heterozygosity

The *MEN1* gene sequence in the blood and tissue DNA was analyzed for mutations by the direct nucleotide sequencing of PCR-amplified exons as described previously [14]. In a MEN1 patient whose germline mutation was not detectable by the conventional sequencing method (case 6), a gross deletion involving exon 8 was detected by PCR-based DNA walking (manuscript in preparation). Loss of heterozygosity in the chromosome 11q13 region was examined at the polymorphic DNA marker sites, *PYGM*, *D11S4940* and *D11S4946*, as described previously [15]. In addition, reduction of the wild type sequence in the tumor DNA at the site of heterozygous germline mutation was also considered as LOH.

Results

Effects of knockdown and overexpression of menin on caspase 8 expression in human cell lines

Because menin knockdown has been shown to suppress caspase 8 expression in murine cells, we examined the effect of menin on caspase 8 expression in human cell lines derived from normal fibroblasts.

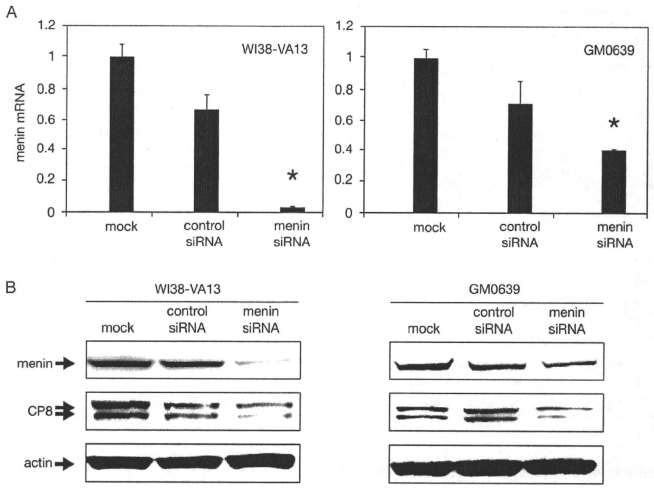

Fig. 1 Caspase 8 expression in menin knockdown experiments. Cells were transfected with control siRNA or menin siRNA or treated with transfection reagents without RNA (mock). (A) The amounts of menin mRNA measured by quantitative RT-PCR in WI38-VA13 (left) and GM0639 (right) cells. Data are presented as the relative value to the mean value of mock-transfected cells and the standard error from three experiments. *, $p<0.05$ versus cells transfected with control siRNA (n=3). (B) Representative Western blot of menin and caspase 8 (CP8) in WI38-VA13 (left) and GM0639 (right) cells. Actin was served as a loading control.

Introduction of menin siRNA into WI38-VA13 and GM0639 cells reduced the menin mRNA and protein levels (Fig. 1). The caspase 8 expression levels were also decreased in the both cell lines by the transfection of menin siRNA (Fig. 1). On the other hand, menin overexperssion in WI38-VA13, GM0639 and HEK293T cells by the transfection of menin expression plasmid did not change procaspase 8 protein levels (Fig. 2). These findings suggest that menin is crucial for caspase 8 expression and that these cells contain sufficient amount of endogenous menin which allow full expression of procaspase 8 protein.

***MEN1* gene status in parathyroid tumors**

In order to examine the effect of menin in human tumors, parathyroid tumors surgically removed from patients affected with MEN1 were used as tumors lacking menin (Table 1). The blood DNA analysis confirmed the presence of germline mutations in all the MEN1 patients except for case 3 whose blood was not available for this study. Comparison of blood and tumor DNA sequences and polymorphic markers revealed LOH in all tumors from the MEN1 patients except for case 3. In the tumor DNA of case 3, which showed the typical manifestations of MEN1 with positive family history of endocrine tumors, the mutated sequence TAG at codon 358 was predominant and the wild type sequence GAG was almost absent (data not shown). These findings suggest that the nonsense mutation E358X (GAG>TAG) is the germline mutation of this family and that the wild-type allele was lost in the tumor cells although it is theoretically possible that a large genomic deletion is the germline mutation of this family and that E358X is a somatic mutation. Altogether, the absence of the normal *MEN1* gene was confirmed in the neoplastic cells of all the tumors from the MEN1 patients examined.

Sporadic parathyroid tumors were used as counterpart specimens, which had normal *MEN1* alleles (Table 1). Because *MEN1* gene inactivation is also

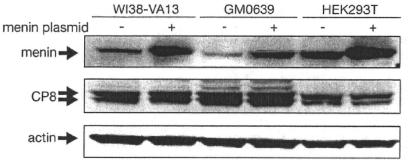

Fig. 2 Menin and caspase 8 (CP8) expression detected by Western blotting in WI38-VA13, GM0639 and HEK293T cells transfected with menin-expressing plasmid (+) or vehicle (-). Actin was served as a loading control.

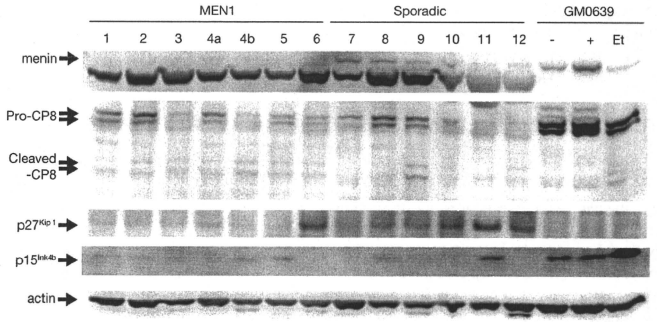

Fig. 3 Menin, caspase 8, $p27^{Kip1}$ and $p15^{Ink4b}$ expression detected by Western blotting in human parathyroid tumors. The samples in lanes 1 - 6 and lanes 7 – 12 are tumors from the MEN1 patients and sporadic tumors, respectively, and correspond to those summarized in Table 1. GM0639 cells transfected with menin-expressing plasmid (+) along with non-transfected cells (-) were used as the size marker for normal menin. GM0639 cells treated with etoposide (Et) were used as the size marker for procaspase 8 (Pro-CP8) and cleaved caspase 8 (Cleaved-CP8). Actin was served as a loading control.

involved in a subset of sporadic parathyroid tumors, we selected only the tumors that had no detectable *MEN1* gene mutation. In order to minimize the possibility of including tumors having *MEN1* gene mutation that escape detection in our mutation analysis, we further selected sporadic tumors that exhibited at least one heterozygous normal polymorphic sequences at codon 418 (GAC/GAT) or codon 541 (GCA/ACA) [1], which are usually hemizygous in tumors involving *MEN1* gene inactivation.

Menin, caspase 8 and CDKI protein levels in parathyroid tumors

Western blotting analyses confirmed that menin protein levels were markedly reduced in parathyroid tumors from MEN1 patients compared with sporadic tumors although some variability was observed (Fig. 3). The faint band of menin with the authentic size detected in the MEN1 tumors should represent menin protein in the non-neoplastic cells in the tumor tissue.

Procaspase 8 protein levels were much more variable among tumors, and there was no constant correlation between menin and procaspase 8 levels (Fig. 3). The cleaved caspase 8 also showed variable expression levels. Even the individual tumors from the same patient (4a and 4b) showed different caspase 8 expression levels. These findings suggest that, while reduction of menin causes decreased procaspase 8 expression in human culture cells *in vitro*, the procaspase 8 and cleaved caspase 8 protein levels in human parathyroid tumors are not simply determined by menin

expression levels but also regulated by other unknown mechanisms.

The expression levels of CDKIs $p27^{Kip1}$ and $p15^{Ink4b}$ were also examined (Fig. 3). The amount of $p27^{Kip1}$ was reduced in all tumors from MEN1 patients except for one case (case 6) while only one case (case 7) of sporadic tumor showed reduced $p27^{Kip1}$ expression. Thus, the expression of $p27^{Kip1}$ was roughly correlated with menin expression levels. On the other hand, the expression of $p15^{Ink4b}$ was not related to *MEN1* gene mutation status. We also attempted to compare $p18^{Ink4c}$ and $p21^{Cip1}$ expression levels in these tumors but failed to detect reproducible specific signals.

Discussion

Menin has been reported to up-regulate the expression of caspase 8 by activating gene transcription and enhance apoptosis in murine fibroblasts [9]. It has also been demonstrated that caspase 8 expression is reduced in the pancreatic islet tumors occurring in the heterozygous *MEN1* gene knockout mice, the murine model of the human MEN1 syndrome [10]. However, caspase 8 expression has not been examined in the human endocrine tumors, in which the *MEN1* gene is completely inactivated. We compared caspase 8 and menin expression levels in human parathyroid tumors from patients affected with MEN1 and non-hereditary, sporadic hyperparathyroidism, and found that caspase 8 protein levels were not correlated with menin protein levels in these tumors.

The discrepancy is not probably due to the species difference because our *in vitro* experiments employing human cells reproduced menin-dependent caspase 8 expression similar to the previous findings with the murine cells. It is also unlikely that an aberrant caspase 8 gene expression is simply associated with oncogenic transformation of endocrine cells because caspase 8 levels have been shown to decline in the murine pancreatic islet tumors lacking menin [10], although the difference of the cell lineage might explain the discrepancy. Examination of human pancreatic islet tumors with verified *MEN1* gene mutations may clarify this possibility.

Another possibility of the apparent discrepancy is the difference of the tumor environments. It is suggested that the basal caspase 8 expression levels are controlled through signals culminating in the activation of SP1 and ETS-like transcription factors [11]. Interferon gamma and retinoic acids have been reported to induce caspase 8 expression in some tumor cell lines [11]. Such extracellular signals may be involved in the regulation of parathyroid cell growth and apoptosis under the physiological condition, and leading to variable caspase 8 expression levels. The distinct caspase 8 expression patterns in the individual tumors form the same patient (4a and 4b) (Fig. 3) may reflect the difference of tumor microenvironment. Alternatively, genetic or epigenetic change of the caspase 8 gene might explain the variable expression. Caspase 8 gene has been shown to be deleted in neuroblastoma [16]. In addition, caspase 8 gene is frequently inactivated by silencing through DNA methylation in various tumors including neuroblastoma and lung carcinoma [11, 16]. The human parathyroid tumors are usually diagnosed and removed after long periods of tumor growth, while tumors developed in the knockout mice were examined earlier, usually less than a year after birth. Therefore, alterations of the caspase 8 gene *per se* might be more prevalent in human tumors than in the murine models. Our present study revealed complex caspase 8 expression patterns in human tumors that may not simply reflect the phenomenon observed under experimental conditions.

In contrast to caspase 8 expression, $p27^{Kip1}$, which was also demonstrated to be up-regulated by menin at the transcriptional level [6], was more abundant in sporadic parathyroid tumors than in tumors from MEN1 patients. These findings are consistent with those reported previously [6] and support the important role of menin in regulating $p27^{Kip1}$ expression. Interestingly, we found no correlation of $p15^{Ink4b}$ protein levels with *MEN1* gene mutation status. The expression of $p15^{Ink4b}$ has also been shown to be up-regulated by menin [17]. However, the previous chromatin immunoprecipitation studies suggested that the enhancing effect of menin on $p15^{Ink4b}$ gene expression may be indirect in contrast to that on $p27^{Kip1}$ gene, which is likely to be regulated through direct binding of menin-containing protein complex to the gene promoter region [17]. Our findings are in line with the previous report that $p15^{Ink4b}$ mRNA levels were not correlated with *MEN1* gene mutation status in human pancreatic endocrine tumors [18]. The $p15^{Ink4b}$ gene promoter hypermethylation has also been demonstrated to be associated with gene silencing in some endocrine tumors [18].

In conclusion, we observed coordinated expression of $p27^{Kip1}$ and menin in human parathyroid tumors but variable expression levels of caspase 8 and $p15^{Ink4b}$ irrespectively of *MEN1* gene mutation status. Because caspase 8 is a crucial component in the apoptosis pathway, low caspase 8 expression is implicated in the resistance against apoptosis-inducing therapy of tumors [11]. Our findings suggest that the human endocrine tumors lacking menin may not always exhibit lower caspase 8 protein expression and hence may not be resistant to such therapy.

Acknowledgments

This study was supported in part by a Grant in-Aid for the Third Comprehensive 10-Year Strategy for Cancer Control and for Cancer Research (21-8-6) from the Ministry of Health, Labour and Welfare of Japan.

References

1. Chandrasekharappa SC, Guru SC, Manickam P, Olufemi SE, Collins FS, Emmert-Buck MR, Debelenko LV, Zhuang Z, Lubensky IA, Liotta LA, Crabtree JS, Wang Y, Roe BA, Weisemann J, Boguski MS, Agarwal SK, Kester MB, Kim YS, Heppner C, Dong Q, Spiegel AM, Burns AL, Marx SJ (1997) Positional cloning of the gene for multiple endocrine neoplasia-type 1. *Science* 276: 404-407.
2. Tsukada T, Nagamura Y, Ohkura N (2009) MEN1 gene and its mutations: Basic and clinical implications. *Cancer Sci* 100: 209-215.
3. Heppner C, Kester MB, Agarwal SK, Debelenko LV, Emmert-Buck MR, Guru SC, Manickam P, Olufemi SE, Skarulis MC, Doppman JL, Alexander RH, Kim YS, Saggar SK, Lubensky IA, Zhuang Z, Liotta LA, Chandrasekharappa SC, Collins FS, Spiegel AM, Burns AL, Marx SJ (1997) Somatic mutation of the *MEN1* gene in parathyroid tumours. *Nat Genet* 16: 375-378.
4. Guru SC, Goldsmith PK, Burns AL, Marx SJ, Spiegel AM, Collins FS, Chandrasekharappa SC (1998) Menin, the product of the *MEN1* gene, is a nuclear protein. *Proc Natl Acad Sci USA* 95: 1630-1634.
5. Maruyama K, Tsukada T, Hosono T, Ohkura N, Kishi M, Honda M, Nara-Ashizawa N, Nagasaki K, Yamaguchi K (1999) Structure and distribution of rat menin mRNA. *Mol Cell Endocrinol* 156: 25-33.
6. Milne TA, Hughes CM, Lloyd R, Yang Z, Rozenblatt-Rosen O, Dou Y, Schnepp RW, Krankel C, Livolsi VA, Gibbs D, Hua X, Roeder RG, Meyerson M, Hess JL (2005) Menin and MLL cooperatively regulate expression of cyclin-dependent kinase inhibitors. *Proc Natl Acad Sci USA* 102: 749-754.
7. Pellegata NS, Quintanilla-Martinez L, Siggelkow H, Samson E, Bink K, Höfler H, Fend F, Graw J, Atkinson MJ (2006) Germ-line mutations in p27Kip1 cause a multiple endocrine neoplasia syndrome in rats and humans. *Proc Natl Acad Sci USA* 103: 15558-15563.
8. Agarwal SK, Mateo CM, Marx SJ (2009) Rare germline mutations in cyclin-dependent kinase inhibitor genes in multiple endocrine neoplasia type 1 and related states. *J Clin Endocrinol Metab* 94: 1826-1834.
9. Schnepp RW, Mao H, Sykes SM, Zong WX, Silva A, La P, Hua X (2004) Menin induces apoptosis in murine embryonic fibroblasts. *J Biol Chem* 279: 10685-10691.
10. La P, Yang Y, Karnik SK, Silva AC, Schnepp RW, Kim SK, Hua X (2007) Menin-mediated caspase 8 expression in suppressing multiple endocrine neoplasia type 1. *J Biol Chem* 282: 31332-31340.
11. Fulda S (2009) Caspase-8 in cancer biology and therapy. *Cancer Lett.* 281: 128-133.
12. Xue L, Yu D, Furusawa Y, Cao J, Okayasu R, Fan S (2009) ATM-dependent hyper-radiosensitivity in mammalian cells irradiated by heavy ions. *Int J Radiat Oncol Biol Phys* 75: 235-243.
13. Xue L, Yu D, Furusawa Y, Okayasu R, Tong J, Cao J, Fan S (2009) Regulation of ATM in DNA double strand break repair accounts for the radiosensitivity in human cells exposed to high linear energy transfer ionizing radiation. *Mutat Res* 670: 15-23.
14. Shimizu S, Tsukada T, Futami H, Ui K, Kameya T, Kawanaka M, Uchiyama S, Aoki A, Yasuda H, Kawano S, Ito Y, Kanbe M, Obara T, Yamaguchi K (1997) Germline mutations of the *MEN1* gene in Japanese kindred with multiple endocrine neoplasia type 1. *Jpn J Cancer Res* 88: 1029-1032.
15. Kishi M, Tsukada T, Shimizu S, Futami H, Ito Y, Kanbe M, Obara T, Yamaguchi K (1998) A large germline deletion of the *MEN1* gene in a family with multiple endocrine neoplasia type 1. *Jpn J Cancer Res* 89: 1-5.
16. Teitz T, Wei T, Valentine MB, Vanin EF, Grenet J, Valentine VA, Behm FG, Look AT, Lahti JM, Kidd VJ (2000) Caspase 8 is deleted or silenced preferentially in childhood neuroblastomas with amplification of MYCN. *Nat Med* 6: 529-535.
17. Karnik SK, Hughes CM, Gu X, Rozenblatt-Rosen O, McLean GW, Xiong Y, Meyerson M, Kim SK (2005) Menin regulates pancreatic islet growth by promoting

histone methylation and expression of genes encoding $p27^{Kip1}$ and $p18^{INK4c}$. *Proc Natl Acad Sci USA* 102: 14659-14664.

18. Lindberg D, Akerström G, Westin G (2008) Evaluation of CDKN2C/p18, CDKN1B/p27 and CDKN2B/p15 mRNA expression, and CpG methylation status in sporadic and MEN1-associated pancreatic endocrine tumours. *Clin Endocrinol* 68: 271-277.
19. den Dunnen JT, Antonarakis SE (2000) Mutation nomenclature extensions and suggestions to describe complex mutations: a discussion. *Hum Mutat* 15: 7-12.
20. Wada S, Watanabe M, Tsukada T, Yasuda S, Yamaguchi K, Kitahama S, Iitaka M, Katayama S (2001) A germline mutation, 1001delC, of the multiple endocrine neoplasia type 1 (*MEN 1*) gene in a Japanese family. *Intern Med* 40: 499-505.
21. Naito J, Kaji H, Sowa H, Kitazawa R, Kitazawa S, Tsukada T, Hendy GN, Sugimoto T, Chihara K (2006) Expression and functional analysis of menin in a multiple endocrine neoplasia type 1 (MEN1) patient with somatic loss of heterozygosity in chromosome 11q13 and unidentified germline mutation of the *MEN1* gene. *Endocrine* 29: 485-490.

Hindawi Publishing Corporation
International Journal of Peptides
Volume 2010, Article ID 305192, 8 pages
doi:10.1155/2010/305192

Review Article

Ghrelin, Des-Acyl Ghrelin, and Obestatin: Regulatory Roles on the Gastrointestinal Motility

Mineko Fujimiya,[1] Akihiro Asakawa,[2] Koji Ataka,[1,3] Chih-Yen Chen,[4] Ikuo Kato,[5] and Akio Inui[2]

[1] *Department of Anatomy, Sapporo Medical University School of Medicine, Sapporo 060-8556, Japan*
[2] *Department of Behavioral Medicine, Kagoshima University Graduate School of Medical and Dental Sciences, Kagoshima 890-8520, Japan*
[3] *Research Institute, Taiko Pharmaceutical Co., Ltd., Osaka 564-0032, Japan*
[4] *Department of Internal Medicine, Faculty of Medicine, National Yang-Ming University School of Medicine, Taipei 112, Taiwan*
[5] *Department of Bioorganic Chemistry, Faculty of Pharmaceutical Sciences, Hokuriku University, Kanazawa 920-1181, Japan*

Correspondence should be addressed to Mineko Fujimiya, fujimiya@sapmed.ac.jp

Received 14 October 2009; Accepted 22 December 2009

Academic Editor: Serguei Fetissov

Ghrelin, des-acyl ghrelin, and obestatin are derived from a common prohormone, preproghrelin by posttranslational processing, originating from endocrine cells in the stomach. To examine the regulatory roles of these peptides, we applied the manometric measurement of gastrointestinal motility in freely moving conscious rat or mouse model. Ghrelin exerts stimulatory effects on the motility of antrum and duodenum in both fed and fasted state of animals. Des-acyl ghrelin exerts inhibitory effects on the motility of antrum but not on the motility of duodenum in the fasted state of animals. Obestatin exerts inhibitory effects on the motility of antrum and duodenum in the fed state but not in the fasted state of animals. NPY Y2 and Y4 receptors in the brain may mediate the action of ghrelin, CRF type 2 receptor in the brain may mediate the action of des-acyl ghrelin, whereas CRF type 1 and type 2 receptors in the brain may mediate the action of obestatin. Vagal afferent pathways might be involved in the action of ghrelin, but not involved in the action of des-acyl ghrelin, whereas vagal afferent pathways might be partially involved in the action of obestatin.

1. Introduction

Ghrelin, des-acyl ghrelin, and obestatin are derived from a prohormone, preproghrelin by posttranslational processing. Ghrelin was first identified as endogenous ligand for growth hormone secretagogue receptors (GHS-R) with O-n-octanoyl acid modification at serine 3 position [1]. Des-acyl ghrelin, on the other hand, has the same amino acid sequence with no O-n-octanoyl acid modification [1]. Obestatin was found by a bioinformatics approach to be encoded by preproghrelin [2]. Obestatin was initially reported to be endogenous ligand for orphan G protein-coupled receptor GPR39 [2]; however recent studies have found no specific binding of obestatin to various types of GPR39-expressing cells [3–5]. Ghrelin is a potent stimulator of food intake and gastrointestinal motility [6], while des-acyl ghrelin exerts opposite effects on food intake and gastrointestinal motility [7]. The effects of obestatin on food intake and gastrointestinal motility have been controversial [8–13].

Recently we developed conscious rat and mouse models to measure physiological fed and fasted motor activities in the gastrointestinal tracts [14–18]. By using these models we succeeded to examine the effects of ghrelin, des-acyl ghrelin, and obestatin on gastroduodenal motility and involvement of hypothalamic peptides mediating the action of these peptides. In this review, we overview the different effects of ghrelin, des-acyl ghrelin, and obestatin on the upper gastrointestinal motility with special attention being paid to brain-gut interactions.

FIGURE 1: Localization of ghrelin, des-acyl ghrelin and obestatin in the rat stomach. (a) Immunofluorescence double staining for acyl ghrelin- (red) and des-acyl ghrelin-positive (green) reaction in the antral mucosa of rat stomach. Acyl ghrelin-positive reaction and des-acyl ghrelin-positive reaction are colocalized in closed-type cells (arrows), whereas des-acyl ghrelin-positive reaction is localized in open-type cells (arrowheads). (b) Immunofluorescence triple staining for des-acyl ghrelin (green), acyl ghrelin (red) and obestatin (blue) in the antral mucosa of rat stomach. Three peptides are colocalized in the closed-type cells (arrows). Bars = 10 μm.

2. Localization of Ghrelin, Des-Acyl Ghrelin, and Obestatin in the Rat Stomach

The localization of ghrelin in the stomach has been studied in various animals by using the specific antibody for ghrelin [19, 20]; however, the localization of des-acyl ghrelin in the stomach has been scarcely examined. We developed antibodies specific for ghrelin (antirat octanoyl ghrelin (1-15) -cys-KLH serum) and for des-acyl ghrelin (antirat des-octanoyl ghrelin (1-15) -cis-KLH serum) and successfully detected the different localization of ghrelin and des-acyl ghrelin in the rat stomach [21].

Both ghrelin- and des-acyl ghrelin-immunoreactive cells were distributed in the oxyntic and antral mucosa of the rat stomach, with higher density in the antral mucosa than oxyntic mucosa. Immunofluorescence double staining showed that ghrelin- and des-acyl ghrelin-positive reactions overlapped in closed-type round cells, whereas des-acyl ghrelin-positive reaction was found in open-type cells in which ghrelin was negative (Figure 1(a)). Ghrelin/des-acyl ghrelin-positive closed-type cells contain obestatin (Figure 1(b)); on the other hand des-acyl ghrelin-positive open-type cells contain somatostatin [21].

The characteristic features of open-type cells that contain des-acyl ghrelin and closed-type cells that contain ghrelin indicate that they may respond differently to intraluminal factors. It is highly possible that open-type cells may react to luminal stimuli more than closed-type cells. Therefore we investigated the effects of different intragastric pH levels on the release of ghrelin and that of des-acyl ghrelin from the ex vivo perfused rat stomach [21]. In a preliminary study we measured the intragastric pH levels in the fasting and fed states of rats and found that intragastric pH in the fasting state was pH 4, whereas that in the fed state was pH 2 [16]. Our results showed that the release of ghrelin was not affected by intragastric pH, whereas the release of des-acyl ghrelin was increased at intragastric pH 2 compared to that at intragastric pH 4 [21]. This result suggests that des-acyl ghrelin-containing cells may sense the intragastric pH via their cytoplasmic processes and release the peptide in accordance with the lower intragastric pH. The fact that the release of des-acyl ghrelin is stimulated by lower intragastric pH seems reasonable because des-acyl ghrelin may act as a satiety signal [6, 7] in the fed state of animals.

3. Manometric Measurement of Gastrointestinal Motility in Conscious Mice and Rats

We developed freely moving conscious animal model to measure the gastrointestinal motility in rats [15] and mice [18]. This model permits the measurement of gastrointestinal motility in animals in the physiological fed and fasted states by a manometric method [15, 18]. In the fasted state, the cyclic changes of pressure waves were detected in both antrum and duodenum, including the quiescence period during which relatively low amplitude contractions occur (phase I-like contractions), followed by a grouping of strong contractions (phase III-like contractions). The frequencies of phase III-like contractions in the fasted motility in the antrum and duodenum in mice (6.0 ± 0.2/h and 6.0 ± 0.3/h, resp.) were significantly ($P < .05$) higher than those in rats (5.3 ± 0.5/h, 5.6 ± 0.8/h, resp.) [15, 18]. After food intake, such fasted motor pattern was disrupted and replaced by a fed motor pattern, which consisted of irregular contractions of high frequency.

4. Ghrelin and Gastroduodenal Motility

Intracerebroventricular (i.c.v.) and intravenous (i.v.) injection of ghrelin stimulated the % motor index (%MI) in the antrum and induced the fasted motor activity in the duodenum when given in the fed state of animals [16, 18] (Figure 2(a)). I.c.v. and i.v. injection of ghrelin increased the frequency of phase III-like contractions in both antrum and duodenum when given in the fasted state of animals [16]. The effects of i.v. injection of ghrelin on gastroduodenal motility were blocked by i.v. injection of GHS-R antagonist but not by i.c.v. injection of GHS-R antagonist [16]. Immunoneutralization of NPY in the brain blocked the stimulatory effects of ghrelin on the gastroduodenal motility [16] (Figure 2(b)). These results indicate that ghrelin released from the stomach may act on the ghrelin receptor on vagal afferent nerve terminals and NPY neurons in the brain may mediate the action of ghrelin on the gastroduodenal motility (Figures 2(c) and 2(d)). Our previous study showed that immunoneutralization of NPY in the brain completely blocked the phase III-like contractions in the duodenum of normal rats, and Y2 and Y4 receptor agonists induced the phase III-like contractions in the duodenum when given in the fed state of animals [15]. Combined together, in normal animals ghrelin may stimulate gastroduodenal motility by activating the GHS-R on vagal afferent nerve terminals and affect NPY neurons in the hypothalamus, and Y2 and/or Y4 receptors in the brain may mediate the action of ghrelin (Figure 2(d), Table 1). Once the brain mechanism is eliminated by truncal vagotomy, ghrelin might be primarily involved in the regulation of fasted molility through GHS-R on the stomach and duodenum [16].

Human ghrelin has a structural resemblance to human motilin, and human ghrelin receptors exhibit a 50% identity with human motilin receptors [22]. Therefore the role of ghrelin in the gastrointestinal motility is comparable with that of motilin [23, 24]. Motilin originates from the endocrine cells in the duodenum [23], while ghrelin originates from the endocrine cells in the stomach [20]; both of them are involved in the regulation of phase III contractions in the gastrointestinal tracts. Motilin induces fasted motility in the stomach and duodenum when it is given peripherally but not when given centrally [24, 25], while ghrelin induces fasted motility in the duodenum when it is given both peripherally and centrally [16]. Since it is known that gastric acidification modulates the action of motilin [26], we examined the relationship between the effects of ghrelin on gastroduodenal motility and intragastric pH. The results showed that within 30 minutes after feeding low intragastric pH (pH 2.5 ± 0.2) inhibited the effects i.v. injected ghrelin on gastroduodenal motility, and that this effect was reversed by an increase of intragastric pH (pH 5.4 ± 0.6) within 60 minutes after feeding, or by pretreatment of famotidine (intragastric pH 6.0–6.7) [16]. These results suggest that the sensitivity of the GHS-R in the gastrointestinal tract might be inhibited by low intragastric pH.

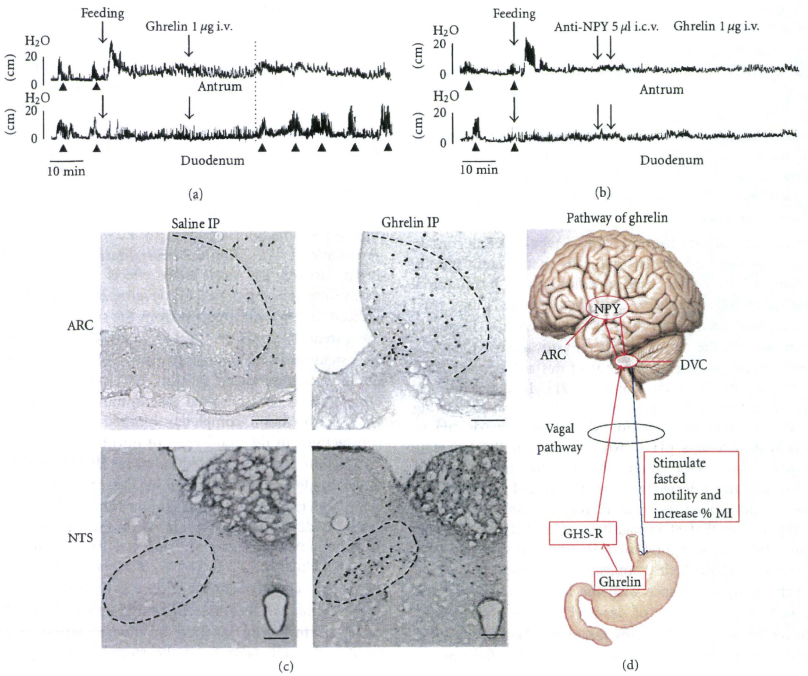

FIGURE 2: Effects of ghrelin on the gastroduodenal motility. (a) Effects of i.v. injection of ghrelin on the fed motor activity of the antrum and duodenum. I.v. injection of ghrelin induces the fasted pattern in the duodenum and increases the motor activity in the antrum. (b) I.c.v. injection NPY antiserum completely blocks the effect of i.v. injection of ghrelin. (c) The density of c-*Fos*-positive cells in the arcuate nucleus (ARC) and NTS is increased by i.p. injection of ghrelin compared to saline-injected control. (d) Summary diagram of the effects of ghrelin on the gastroduodenal motility and brain mechanism mediating its action.

TABLE 1: Summary of the regulatory roles of ghrelin, des-acyl ghrelin and obestatin on the gastroduodenal motility.

	ghrelin		des-acyl ghrelin		obestatin	
	Fasted state	Fed state	Fasted state	Fed state	Fasted state	Fed state
Stomach	↑	↑	↓	—	—	↓
Duodenum	↑	↑	—	—	—	↓
Hypothalamic neuron	NPY		urocortin 2		CRF, urocortin 2	
Brain receptor	Y2, Y4		CRF type 2		CRF type 1, type 2	
Vagal afferent pathway	+		—		+	

5. Des-Acyl Ghrelin and Gastroduodenal Motility

Central and peripheral administration of des-acyl ghrelin has been shown to significantly decrease food intake in food-deprived mice and decrease gastric emptying [6]. Transgenic mice with overexpression of the des-acyl ghrelin gene exhibited a decrease in body weight, food intake, and fat mass weight accompanied by moderately decreased linear growth compared with their nontransgenic littermates [6]. In rats, des-acyl ghrelin injected intraperitoneally (i.p.) effectively decreased food intake in food-deprived rats and decreased the dark-phase food intake in free-feeding rats but failed to decrease the light-phase food intake in free-feeding rats [7].

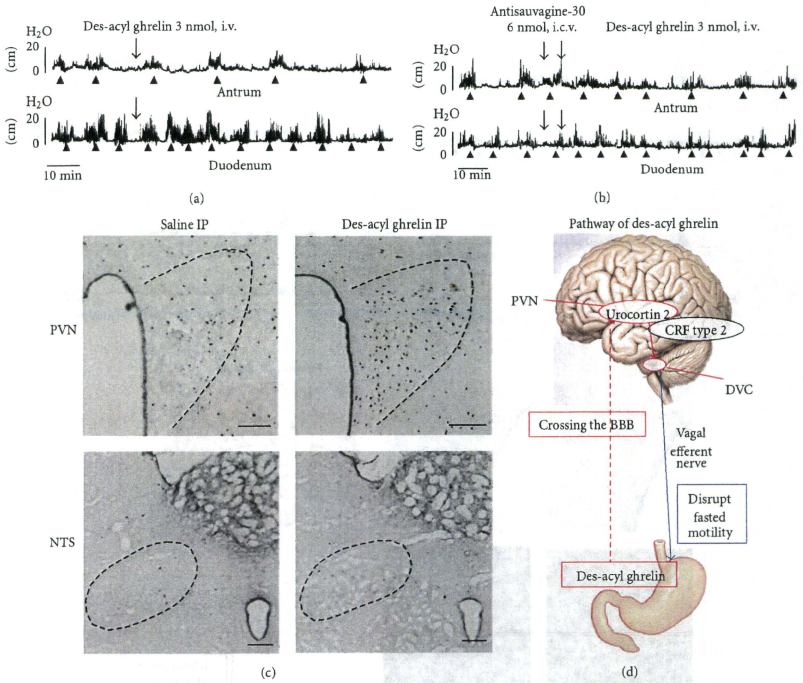

FIGURE 3: Effects of des-acyl ghrelin on the gastroduodenal motility. (a) Effects of i.v. injection of des-acyl ghrelin on the fasted motor activities of the antrum and duodenum. I.v. injection of des-acyl ghrelin decreases the frequency of phase III-like contractions in the antrum but not in the duodenum. (b) The decreased frequency of phase III-like contractions induced by i.v. injection of des-acyl ghrelin is restored to normal in pretreatment of i.c.v. injection of the selective CRF type 2 receptor antagonist antisauvagine-30. (c) The density of c-*Fos*-positive cells in the PVN is increased by i.p. injection of des-acyl ghrelin compared to saline-injected control, whereas that in the NTS is not altered. (d) Summary diagram of the effects of des-acyl ghrelin on the gastroduodenal motility and brain mechanism mediating its action.

I.c.v. and i.v. injections of des-acyl ghrelin disrupted fasted motility in the antrum but not in the duodenum [7] (Figure 3(a)). The frequencies of fasted motility in the antrum were decreased to 58.9% and 54.5% by des-acyl ghrelin injcted i.c.v. and i.v., respectively, [7]. However i.c.v. and i.v. injections of des-acyl ghrelin did not alter fed motor activity in both the antrum and duodenum [7]. These data indicate that the dominant role of exogenous des-acyl ghrelin affects fasted motility in the antrum but not in the duodenum. The results showed that capsaicin treatment did not alter the disruptive effect of i.v. injection of des-acyl ghrelin on fasted motility in the antrum [7]. These results were consistent with electrophysiological studies, which showed that peripheral administration of ghrelin suppressed firing of the vagal afferent pathways, whereas des-acyl ghrelin had no effect on vagal afferent pathways [27]. Difference in the involvement of vagal afferent pathways in the action of ghrelin and des-acy ghrelin was confirmed by c-*Fos* expression in the NTS. I.p. injection of ghrelin significantly increased the density of c-*Fos*-positive cells in the NTS (Figure 2(c)), while i.p. injection of des-acyl ghrelin induced no change in the density of c-*Fos*-positive cells in the NTS compared with vehicle-injected controls [7] (Figure 3(c)). Taken together, these results suggest that peripherally administered des-acyl ghrelin may cross the blood-brain barrier (BBB) and act directly on the brain receptor and disrupt the fasted motility in the antrum (Figure 3(d)).

The centrally administered CRF type 2 receptor antagonist, but not the CRF type 1 receptor antagonist, blocked the effects of centrally and peripherally administered des-acyl ghrelin on gastric motility [7] (Figure 3(b)). Between